Biochimica et Biophysica Acta 1842 (2014) 1556–1566

Contents lists available at ScienceDirect

Biochimica et Biophysica Acta

journal homepage: www.elsevier.com/locate/bbadis

Early alterations in energy metabolism in the hippocampus of APPswe/PS1dE9 mouse model of Alzheimer's disease

Ignacio Pedrós [b,c,h,1], Dmitry Petrov [a,c,h,1], Michael Allgaier [a,c,h], Francesc Sureda [b,c,h], Emma Barroso [a,d,h], Carlos Beas-Zarate [f,g,h], Carme Auladell [e,h], Mercè Pallàs [a,c,h], Manuel Vázquez-Carrera [a,d,h], Gemma Casadesús [f,h], Jaume Folch [b,c,h,2], Antoni Camins [a,c,h,*,2]

[a] Unitat de Farmacologia i Farmacognòsia, Facultat de Farmàcia, Institut de Biomedicina de la UB (IBUB), Universitat de Barcelona, Barcelona, Spain
[b] Unitats de Bioquímica i Farmacologia, Facultat de Medicina i Ciències de la Salut, Universitat Rovira i Virgili, Reus, Tarragona, Spain
[c] Centros de Investigación Biomédica en Red de Enfermedades Neurodegenerativas (CIBERNED), Spain
[d] Centros de Investigación Biomédica en Red de Diabetes y Enfermedades Metabólicas Asociadas (CIBERDEM), Spain
[e] Departament de Biologia Cellular, Facultat de Biologia, Universitat de Barcelona, Barcelona, Spain
[f] Department of Neurosciences, Case Western Reserve University, Cleveland OH USA
[g] Laboratorio de Neurobiología Celular y Molecular, División de Neurociencias, CIBO, IMSS, Mexico
[h] Laboratorio de Regeneración y Desarrollo Neural, Instituto de Neurobiología, Departamento de Biología Celular y Molecular, CUCBA, Mexico

ARTICLE INFO

Article history:
Received 7 February 2014
Accepted 20 May 2014
Available online 2 June 2014

Keywords:
APPswe/PS1dE9
Insulin receptor
Mitochondria
Hippocampus
Tau
Alzheimer's disease

ABSTRACT

The present study had focused on the behavioral phenotype and gene expression profile of molecules related to insulin receptor signaling in the hippocampus of 3 and 6 month-old APPswe/PS1dE9 (APP/PS1) transgenic mouse model of Alzheimer's disease (AD). Elevated levels of the insoluble Aβ (1–42) were detected in the brain extracts of the transgenic animals as early as 3 months of age, prior to the Aβ plaque formation (pre-plaque stage). By the early plaque stage (6 months) both the soluble and insoluble Aβ (1–40) and Aβ (1–42) peptides were detectable. We studied the expression of genes related to memory function (*Arc*, *Fos*), insulin signaling, including insulin receptor (*Insr*), *Irs1* and *Irs2*, as well as genes involved in insulin growth factor pathways, such as *Igf1*, *Igf2*, *Igfr* and *Igfbp2*. We also examined the expression and protein levels of key molecules related to energy metabolism (PGC1-α, and AMPK) and mitochondrial functionality (OXPHOS, TFAM, NRF1 and NRF2). 6 month-old APP/PS1 mice demonstrated impaired cognitive ability, were glucose intolerant and showed a significant reduction in hippocampal *Insr* and *Irs2* transcripts. Further observations also suggest alterations in key cellular energy sensors that regulate the activities of a number of metabolic enzymes through phosphorylation, such as a decrease in the *Prkaa2* mRNA levels and in the pAMPK (Thr172)/Total APMK ratio. Moreover, mRNA and protein analysis reveals a significant downregulation of genes essential for mitochondrial replication and respiratory function, including PGC-1α in hippocampal extracts of APP/PS1 mice, compared to age-matched wild-type controls at 3 and 6 months of age. Overall, the findings of this study show early alterations in genes involved in insulin and energy metabolism pathways in an APP/PS1 model of AD. These changes affect the activity of key molecules like NRF1 and PGC-1α, which are involved in mitochondrial biogenesis. Our results reinforce the hypothesis that the impairments in both insulin signaling and energy metabolism precede the development of AD amyloidogenesis.

1. Introduction

Alzheimer's disease (AD) is the most common cause of senile dementia and the incidence rates of the disease are increasing exponentially due to the amount of aged population. AD diagnosis is based on the detection of senile amyloid-β (Aβ) plaques and neurofibrillary tangles in the brain [1]. Although the exact mechanisms triggering neurodegeneration in AD remain unclear, a number of hypotheses have been proposed [2–11].

In recent years, several studies have focused on the potential relationship between AD and metabolic disorders [14–17]. Obesity and diabetes significantly increase the risks of cognitive decline and AD, suggesting that brain glucose metabolism impairments [18–25] may be linked to AD pathogenesis [14]. Both the AD and type 2 diabetes mellitus (T2DM) are associated with peripheral and central insulin signaling abnormalities, including alterations in brain insulin and insulin-like

* Corresponding author at: Unitat de Farmacologia i Farmacognosia, Facultat de Farmàcia, Universitat de Barcelona, Avda/Diagonal 643, E-08028 Barcelona, Spain. Tel.: +34 93 4024531; fax: +34 934035982.
E-mail address: camins@ub.edu (A. Camins).
[1] These authors contributed equally to this work.
[2] Senior co-authors.

http://dx.doi.org/10.1016/j.bbadis.2014.05.025
0925-4439/

growth factor (IGF) levels [19–22]. Pathological changes in these signaling pathways affect neuronal survival, energy homeostasis, gene expression and memory processes [23–30]. For instance, insulin and IGF1 regulate the expression and phosphorylation of Tau protein through activation of kinases [26–36].

Therefore, AD could be considered as a "type 3 diabetes" metabolic disorder, with insulin providing the link connecting both chronic diseases [19–22]. Several studies have reported a role for insulin in the control of neuronal function in cortical and hippocampal areas, which are involved in memory processing and cognitive functions [24–26]. Thus, insulin directly influences neurons, modulates neurotransmitter release, neuronal outgrowth, neuronal survival, as well as synaptic plasticity [19]. Moreover, it has been demonstrated that soluble Aβ oligomers alter insulin signaling because they bind to insulin receptors in hippocampal neurons, thereby inducing receptor mobilization from the membrane and into the cell [15].

Another molecule implicated both in diabetes and AD is the insulin-degrading enzyme (IDE). IDE is capable of degrading both insulin and Aβ, however it binds insulin with a much higher affinity. In an animal model of T2DM, elevated levels of circulating insulin resulted in competitive inhibition of IDE, thus causing an increase in Aβ levels. Additionally, mice lacking IDE have lower rates of Aβ and insulin degradation, and develop hyperinsulinemia and Aβ deposits in the brain [19–21].

AD etiology is complex and Aβ by itself is unable to account for all aspects of AD [1–6,37–41]. In order to identify the underlying causes of the disease, it is of utmost importance to understand the potential correlations between Aβ oligomers and hippocampal metabolism in early disease-stages, prior to plaque deposition. Most of AD research is currently undertaken in animal models that have increased Aβ levels compared to controls, and while Aβ pathology is mimicked in these models, many other factors associated with AD are not. Transgenic mice that carry an APP and presenilin 1 (PS1) mutations show AD-like pathology and memory impairment, and are useful for studying AD and testing possible treatments [42]. The current study, carried out in an APP/PS1 model of AD, aimed to identify the metabolic pathways responsible for the onset of AD, with the main focus on the early disease-stages, prior to the formation of senile plaques and memory loss. For this purpose, we examined behavioral phenotype and mRNA expression and protein levels of genes related to insulin receptor and mitochondria signaling in 3 and 6 month-old APP/PS1 mice. Three month-old animals were chosen because at this age, neither significant cognitive loss, nor brain Aβ plaques are detectable compared to the six month-old mice, which exhibit high brain Aβ content and memory loss [12–14].

2. Materials and methods

2.1. Animals

Male APPswe/PS1dE9 and C57BL/6 mice were used in this study. APP/PS1 animals co-express a Swedish (K594M/N595L) mutation of a chimeric mouse/human APP (Mo/HuAPP695swe), together with the human exon-9-deleted variant of PS1 (PS1-dE9), allowing these mice to secrete elevated amounts of human Aβ peptide. Both mutations are associated with AD, are under control of the mouse prion protein promoter, directing both mutated proteins mainly to the CNS neurons, and result in age-dependent amyloid plaque depositions in mouse brain. The APPswe-mutated APP is a favorable substrate for β-secretase, whereas the PS1dE9 mutation alters β-secretase cleavage, thereby promoting overproduction of Aβ42. The animals were kept under controlled temperature, humidity and light conditions with food and water provided ad libitum. Mice were treated in accordance with the European Community Council Directive 86/609/EEC and the procedures established by the Department d'Agricultura, Ramaderia i Pesca of the Generalitat de Catalunya. Every effort was made to minimize animal suffering and to reduce the number of animals used. Fifty animals, divided into four groups, were used for the present study, with at least 10 wild-type and 10 APP/PS1 transgenic mice of 3 and 6 months of age, per group. Following in vivo testing, the animals were sacrificed and at least 6 mice in each group were used for RNA and protein extract isolation, with an additional 4 mice for immunohistochemistry.

2.2. Glucose and insulin tolerance tests

Intraperitoneal glucose tolerance tests (IP-GTT) and insulin tolerance tests (ITT) were performed in accordance with the previously published guidelines [72]. For IP-GTT, mice were fasted overnight for 16 h. The test was performed in a quiet room, preheated to +30 °C. The tip of the tail was cut with the heparin-soaked (Heparina Rovi, 5000 IU/ml; Rovi S.A.; Madrid, Spain) scissors, 30 min prior to 1 g/kg intraperitoneal glucose injection (diluted in H_2O). Blood glucose levels of the tail vein were measured at −30, 0, 5, 15, 30, 60 and 120 min after the glucose injection with the Ascensia ELITE blood glucose meter (Bayer Diagnostics Europe Ltd.; Dublin, Ireland). ITT was performed in similar conditions with the 0.25 IU/kg of human insulin, diluted in saline (Humulina Regular, 100 IU/ml/Lilly, S.A.; Madrid, Spain), except that the mice underwent a 5-hour morning fast. Blood glucose levels were measured at −30, 0, 15, 30, 45 and 60 min after the insulin administration. If, during this time, blood glucose levels dropped to below 20 mg/dl, 1 g/kg glucose was administered to counteract the effects of insulin, in order to reduce animal suffering.

2.3. Novel object recognition test

The test was conducted as described previously [43] in a 90° two arm, 25 cm long, and 20 cm high maze. The light intensity in the middle of the field was 30 lx. The objects to be discriminated were plastic figures (object A: 5.25 cm high, object B: 4.75 cm high). First, mice were individually habituated to the apparatus for 10 min a day, for two days. On the third day, they were submitted to a 10 min acquisition trial (first trial) during which they were placed in the maze in the presence of two identical novel objects (A + A, or B + B) placed at the end of each arm. A 10 min retention trial, with the objects (A + B) (second trial) occurred 2 h later. The amount of exploration time each animal spent on objects A and B during the acquisition trial varied between 5 and 20 s, depending on the individual mouse. Total exploration time between the 2 objects when calculated for each individual animal indicated the absence of the object preference bias (Fig. 1C) (n = 5–9 per group). During the retention trial, the times that the animal took to explore the new object (tn) and the old object (to) were recorded. A discrimination index (DI) was defined as (tn − to) / (tn + to). In order to avoid further object preference biases, objects A and B were counterbalanced so that half of the animals in each experimental group were first exposed to object A and then to object B, whereas the other half saw first object B and then object A. The maze, the surface, and the objects were cleaned with 96° ethanol between animals, so as to eliminate olfactory cues.

2.4. Immunohistochemistry

For detection of Aβ deposits, free-floating coronal sections, 20 μm thick, were rinsed with 0.1 mol/l PB, pH 7.2, and pre-incubated in 88% formic acid. Then, sections were treated with 5 ml/l H_2O_2 and 100 ml/l methanol in PBS and pre-incubated in a blocking solution (100 ml/l of FBS, 2.5 g/l of BSA and 0.2 mol/l of glycine in PBS with 5 ml/l of Triton X-100). After that, sections were incubated overnight (O/N) at 4 °C with the primary mouse anti-human beta-amyloid clone 6F/3D antibody (1:100; DakoCytomation, Denmark). Then, sections were incubated with the biotinylated secondary antibody (1:200; Sigma-Aldrich) followed by the avidin–biotin–peroxidase complex (ABC; 1:200; Vector, Burlingame, CA). Peroxidase reaction was developed with 0.5 g/l diaminobenzidine in 0.1 mol/l PB and 0.1 ml/l H_2O_2, and immunoreacted

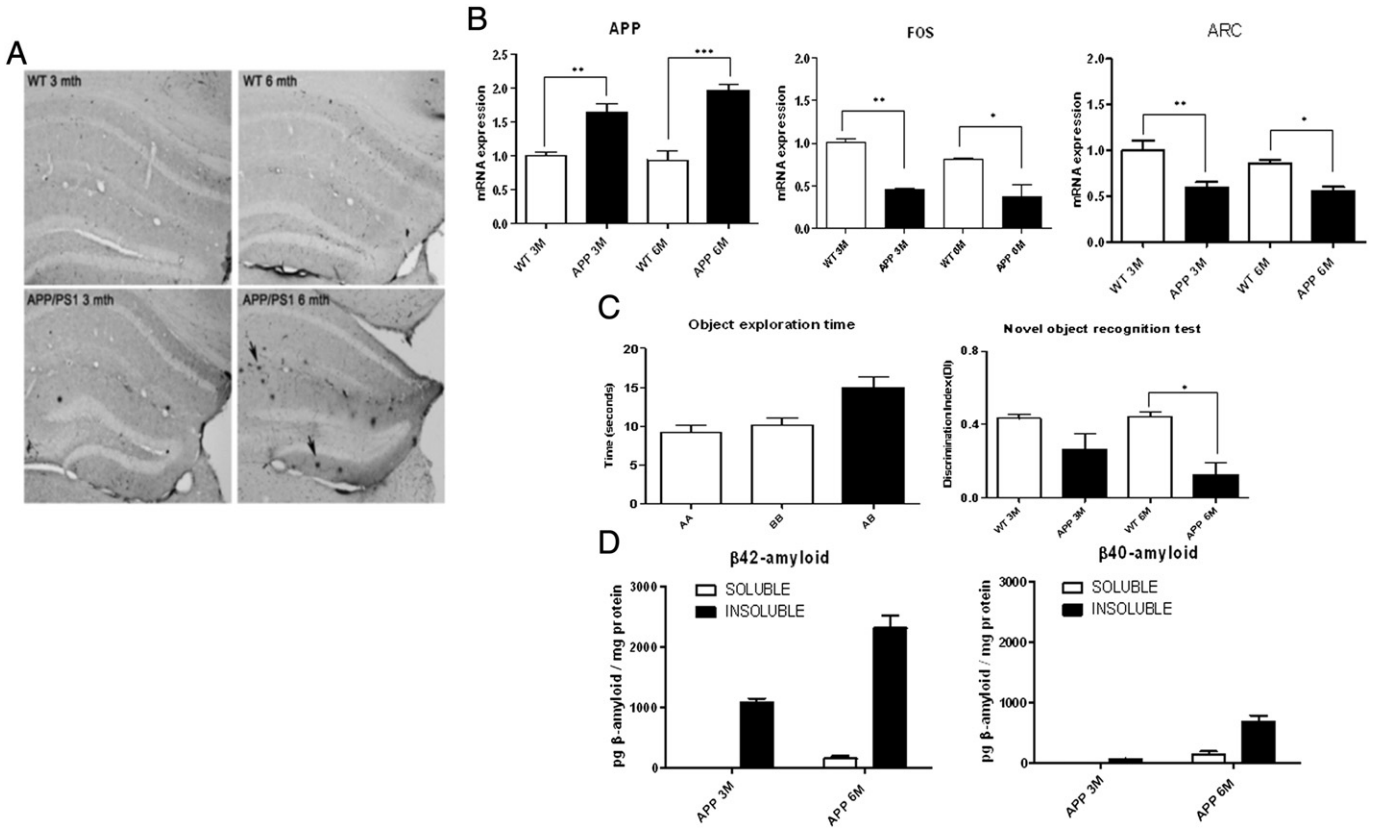

Fig. 1. Representative immunohistochemical staining with the Aβ-specific 6F/3D antibody, in 3 and 6 month-old mice, demonstrating Aβ plaque deposits in the hippocampus of 6 month-old APP/PS1 animals (A). mRNA expression profile of app, fos and Arc in the hippocampal extracts (n = 6) (B). The results of the 2 object novel object recognition test, demonstrating an absence of the object preference bias and a significant memory loss in 6 month-old APP/PS1 animals, compared to wild-type controls (n = 7–12) (C). Concentrations of the soluble and insoluble human Aβ (1–40) and Aβ (1–42) peptides in the cortical extracts in 3 and 6 month-old APP/PS1 mice, expressed as pg/mg of total protein as determined by ELISA (n = 5–6) (D). (Statistical analysis was performed with one-way ANOVA, with Tukey's post-hoc test, where * denotes $p < 0.05$, ** denotes $p < 0.01$, and *** denotes $p < 0.001$.)

sections were mounted on gelatinized slides. Stained sections were examined under a light microscope (Olympus BX61).

2.5. Western blot analysis

Aliquots of hippocampus homogenate containing 15 mg of protein per sample were analyzed using the Western blot method. In brief, samples were placed in a sample buffer (0.5 m Tris–HCl, pH 6.8, 10% glycerol, 2% (w/v) SDS, 5% (v/v) 2-mercaptoethanol, 0.05% bromophenol blue) and denatured by boiling at 95–100 °C for 5 min. Samples were separated by electrophoresis on 10–15% acrylamide gels. Following this, the proteins were transferred to PVDF sheets using transblot apparatus. Membranes were blocked overnight with 5% non-fat milk dissolved in TBS-T buffer (50 mM Tris; 1.5% NaCl, 0.05% Tween 20, pH 7.5). They were then incubated with primary antibodies, as detailed in Table 1. After O/N incubation, blots were washed thoroughly in TBS-T buffer and incubated for 1 h with a peroxidase-conjugated IgG secondary antibody (1:2000). Immunoreactive protein was detected using a chemiluminescence-based detection kit. Protein levels were determined by densitometry, using Chemi doc XRS + Molecular Imager detection system (Bio-Rad), with ImageLab image analysis software. Measurements are expressed as arbitrary units. All results are normalized to GAPDH, unless stated otherwise.

2.6. Serum insulin ELISA

Heart puncture was used to collect whole blood samples from 3 and 6 month-old wild-type and APP/PS1 mice, following a 5-hour morning fast, at the point of sacrifice. Blood samples were transferred to Serum-Gel Z microcentrifuge tubes (Sarstedt, Numbrecht, Germany), for serum separation. The samples were collected and kept at room temperature, and the serum was separated by centrifugation for 10 min at 5000 ×*g*. Serum insulin levels were measured with Rat/Mouse Insulin ELISA kit (Cat #: EZRMI-13K; EMD Millipore; St. Charles, MO, USA), according to manufacturer's instructions, utilizing 10 μl of mouse serum.

Table 1
A list of antibodies used for the immunoblotting experiments.

Protein	Antibody
pAMPK (Thr 172)	#2531 (Cell signaling)
AMPK	#2532 (Cell signaling)
PGC1A	101707 (Cayman chemical)
TFAM	DR1071b (Calbiochem)
NRF1	Sc-28379 (Santa Cruz biotech)
IDE	Ab32216 (Abcam)
pGSK3B (Tyr 216)	Ab74754 (Abcam)
pGSK3B (Ser 9)	#9336 (Cell signaling)
GSK3B	#9315 (Cell signaling)
pCDK5 (Tyr 15)	ab63550 (Abcam)
CDK5	Sc-173 (Santa Cruz biotech)
P35	#2680 (Cell signaling)
pTAU (Ser 199)	44734G (Life Technologies)
pTAU (Thr 205)	44738G (Life Technologies)
pTAU (Ser 396)	44752G (Life Technologies)
pTAU (Ser 404)	44748G (Life Technologies)
TAU5	AHB0042 (Biosource)
PSD-95	Ab18258 (Abcam)
SYP	M0776 (DakoCytomation)
OXPHOS	MS604 (MitoSciences)
GAPDH	MAB374 (Millipore)
2nd–ary Anti-Mouse	170-5047 (Biorad)
2nd–ary Anti-Rabbit	NA934V (GE Healthcare)

2.7. Measurement of Aβ peptides in brain tissues by ELISA

Aβ 1–40 and Aβ 1–42 were measured in cortical extracts according to a previously published procedure [44]. In brief, the samples were weighed and homogenized in a 8× volume of PBS with AEBSF protease inhibitor cocktail set (Cat # 539131; Calbiochem; La Jolla, CA, USA). The soluble fraction was separated by centrifuging the samples for 10 min at 4000 ×*g*. The pellets containing insoluble Aβ peptides were solubilized in a 5 M guanidine HCl/50 mM Tris HCl solution by incubating for 3.5 h on an orbital shaker at room temperature in order to obtain insoluble fraction. The levels of soluble and insoluble Aβ 1–40 and Aβ 1–42 were determined employing the commercially available human ELISA kits (Cat # KHB3481 and KHB3441; Invitrogen, Camarillo, CA, USA). Data obtained from the cortical homogenates are expressed as picograms of Aβ content per milligrams of total protein (pg/mg).

2.8. RNA extraction and quantification

Total RNA was isolated from the hippocampi of wild-type and APP/PS1 transgenic mice, as described previously [73]. Briefly, the tissue was homogenized in the presence of Trizol reagent (Life Technologies Corporation). Chloroform was added and the RNA was precipitated from the aqueous phase with isopropanol at 4 °C. RNA pellet was reconstituted in RNAse-free water, with the RNA integrity determined by Agilent 2100 Bioanalyzer.

2.9. Quantitative RT-PCR

First-strand cDNA was reverse transcribed from 2 μg of total RNA from the hippocampi of 3 and 6 month-old mice, using the High Capacity cDNA Reverse Transcription kit, according to manufacturer's protocol (Applied Biosystems). Equal amounts of cDNA of each individual animal were subsequently used for qRT-PCR, and each sample was analyzed in triplicate for each gene. TaqMan gene expression assays (Applied Biosystems) as detailed in Table 2 were used to determine transcription levels of individual genes. qRT-PCR was performed on the StepOnePlus Real Time PCR system (Applied Biosystems) and normalized to the average transcription levels of gapdh and tbp, using the delta–delta Ct method.

2.10. Statistical analysis

All data are presented as means ± SEM, and differences are considered significant at $p < 0.05$, $p < 0.01$ and $p < 0.001$. Differences between samples/animals were evaluated using either one-way ANOVA, with Tukey's post-hoc test, where * denotes $p < 0.05$, ** denotes $p < 0.01$, and *** denotes $p < 0.001$ and with the student's t-test, where $ denotes $p < 0.05$, $$ denotes $p < 0.01$ and $$$ denotes $p < 0.001$. Both the statistical analyses and the graphs presented here were created with the GraphPad InStat software V5.0 (GraphPad Sofware Inc., San Diego, CA, USA).

Table 2
A list of probes used for qRT-PCR analyses.

Gene	TaqMan probe
app	Mm01344172_m1
arc	Mm00479619_g1
fos	Mm00487425_m1
gapdh	Mm99999915_g1
igf1	Mm01228180_m1
igf2	Mm00439564_m1
igfbp2	Mm00492632_m1
igf1r	Mm00802831_m1
ins1	Mm01950294_s1
insr	Mm01211875_m1
irs1	Mm01278327_m1
irs2	Mm03038438_m1
nrf1	Mm01135606_m1
nfe2l2	Mm00477784_m1
Ppargc1a	Mm01208835_m1
prkaa1	Mm01296700_m1
prkaa2	Mm01264789_m1
tbp	Mm00446971_m1
tfam	Mm00447485_m1

3. Results

3.1. Early phenotypical signs of amyloidogenesis in APP/PS1 mice

In order to determine the extent of the amyloid deposition in the brains of APP/PS1 mice, hippocampal sections were stained with the 6F/3D monoclonal antibody, which is specific for the human form of the Aβ peptide. It was previously reported that the amyloid plaque deposits first start to appear at the age of 6 months in this model [13,14]. In agreement with the earlier studies, our immunohistochemical results demonstrated neither diffuse nor fibrillar plaque deposition in the brains of APP/PS1 mice at 3 months of age. In contrast, Aβ protein aggregates were clearly visible by the age of 6 months (Fig. 1A). In addition, a significant increase in the mRNA levels of the app (utilizing a probe which recognizes both human and mouse transcripts) was detected in hippocampal extracts of both 3 and 6 month-old animals. Likewise, we observed a significant reduction in the mRNA levels of *Arc* and *fos*, which play a role in memory function, in the brains of APP/PS1 mice [45] (Fig. 1B). Moreover, we have characterized the progression of cognitive impairment, utilizing a 2 object novel object recognition test. Our results showed a significant memory loss in 6 month-old APP/PS1 mice (Fig. 1C).

Interestingly, we have detected significant levels of the insoluble Aβ (1–42) peptides in the cortical homogenates of 3 month old APP/PS1 mice (>1000 pg/mg), at an age when Aβ plagues are not yet detectable by immunohistochemistry. The amyloid burden was further increased in 6 month old transgenic animals, with the detectable levels of both soluble and insoluble Aβ (1–40) (>140 and >680 pg/mg) and of soluble and insoluble Aβ (1–42) (>150 and >2300 pg/mg) (Fig. 1D).

3.2. Glucose and insulin tolerance tests and peripheral insulin levels

Since a connection between AD and T2DM has been established during the past decade, we intended to identify any metabolic perturbations in glucose metabolism in the APPswe/PS1dE9 strain [18]. In fact, as shown in Fig. 2, APP/PS1 mice exhibited impaired fasting glucose and insulin tolerance, following IP-GTT and ITT, respectively. Interestingly, the biggest differences in blood glucose levels, between the wild-type and transgenic animals, were detected from 30 to 120 min following i.p. glucose administration in IP-GTT or insulin administration in ITT. In addition, a slight increase in fasting peripheral insulin levels, determined by ELISA, was observed in 6 month-old APP/PS1 mice, compared to age-matched controls. Having confirmed the existence of the peripheral metabolic phenotype in the APP/PS1 mice, we then proceeded to study the expression of genes related to insulin metabolism in the brain, with a particular focus on hippocampal insulin receptor signaling pathway.

3.3. Identification of differentially expressed genes related to insulin receptor

Previous studies demonstrated alterations in brain insulin signaling in AD, but the onset and the severity of this impairment are unclear [43–46]. For this reason, we evaluated mRNA expression of preproinsulin 1 (*Ins1*), insulin receptor (*Insr*), insulin receptor substrates 1 (*Irs1*) and 2 (*Irs2*), insulin-like growth factors I (*Igf1*) and II (*Igf2*), IGF receptor (*Igfr*), as well as insulin-like growth factor-binding protein 2 (igfbp2), at 3 and 6 months of age (Fig. 3). We detected a small, but significant reduction

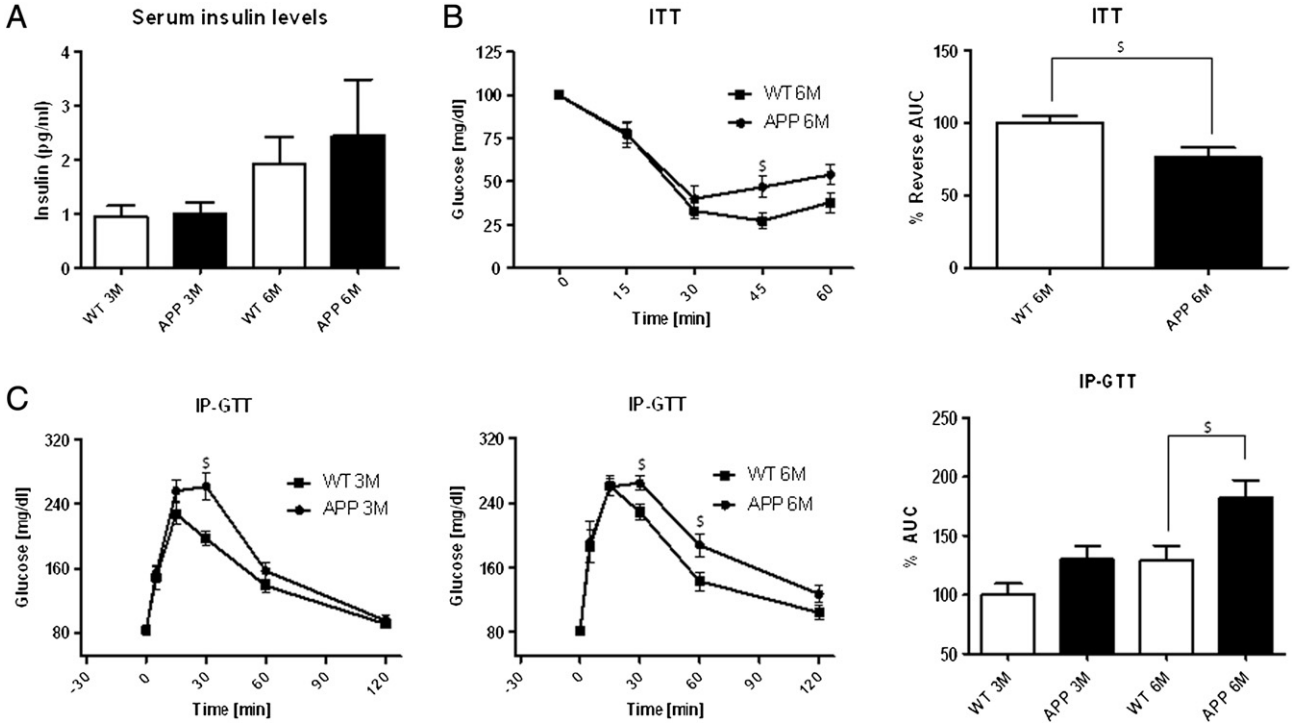

Fig. 2. Fasting serum insulin levels ELISA (n = 5–7) (A), insulin tolerance test (n = 5–7) (B) and intraperitoneal glucose tolerance test (n = 5–12) (C) in 3 and 6 month-old wild-type and APP/PS1 mice. For the ITT and the IP-GTT, AUC data were calculated from the timepoint 0 till the end of the experiment (Statistical analysis was performed with the student's t-test, where $ denotes $p < 0.05$.)

in *insr* and *irs2* transcripts in the hippocampal extracts of 3 month-old APP/PS1 mice, compared to age-matched controls. Interestingly, the expression of both *Igf2* and *Igfbp2* transcripts was significantly increased at 6 months in transgenic animals.

3.4. Energy metabolism is impaired in the early stages of the amyloidogenesis

AMP-activated protein kinase (AMPK) is a sensor of cellular stress that maintains energy homeostasis by promoting mitochondrial

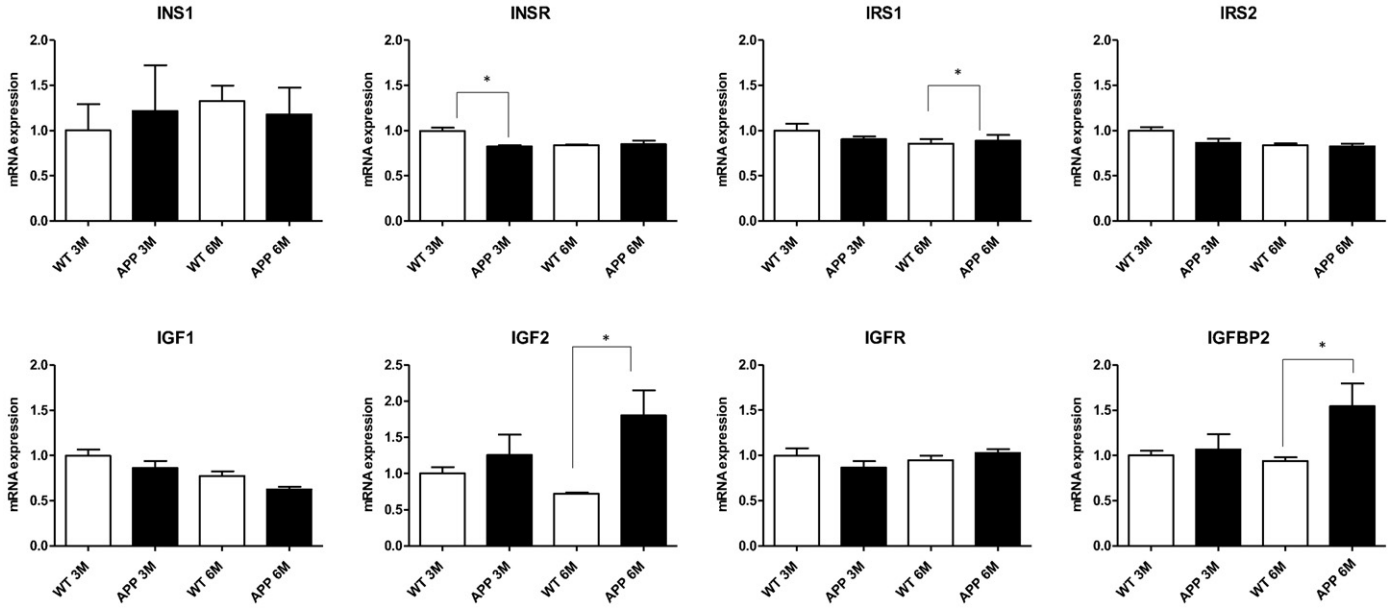

Fig. 3. mRNA expression profile of genes related to insulin signaling pathway in the hippocampal extracts of 3 and 6 month-old wild-type and APP/PS1 mice (n = 4–6). (Statistical analysis was performed with one-way ANOVA and with Tukey's post-hoc test, where * denotes $p < 0.05$.)

biogenesis through transcriptional coactivator peroxisome proliferator activated receptor-γ coactivator 1α (PGC-1α) signaling pathway [47–54]. We detected a significant reduction in the mRNA levels of the alpha 2 (*Prkaa2*), but not of the alpha 1 (*Prkaa1*) isoform of the catalytic subunit of AMPK, in the hippocampi of 3 month-old APP/PS1 mice, compared to wild-type controls (Fig. 4A). This observation is consistent with the slight reduction in the protein levels of phosphorylated AMPK (pAMPK (Thr172)/Total APMK ratio) (Fig. 4B). Thus, our data suggest alterations in a key cellular energy sensor that regulates the activities of a number of molecules involved in cellular metabolism.

PGC-1α is involved in energy homeostasis and glucose metabolism, as well as in mitochondrial metabolism and biogenesis [49,50]. In the current study, we detected a significant reduction in PGC-1α mRNA and protein (Fig. 4) levels in the hippocampi of 3 and 6 month-old APP/PS1 mice, compared to control animals. Since PGC-1α regulates the transcriptional activity of genes essential for mitochondrial replication and respiratory function, such as estrogen-related receptor α (ERR-α), nuclear respiratory factor (NRF) and mitochondrial transcription factor A (TFAM), we proceeded to study their mRNA and protein levels.

3.5. The impairment of mitochondrial biogenesis is involved in the early stages of the amyloidogenesis

It has been hypothesized that mitochondrial dysfunction could be a trigger of AD [49–54]. In fact, mRNA expression analysis of genes, downstream to PGC-1α, confirmed significant reductions in *Nrf1* and *Nrf2* transcripts in the hippocampi of 3-month old APP/PS1 animals, compared to controls. mRNA levels of *Tfam* were also slightly reduced at this age, although the observed changes did not reach statistical significance (Fig. 4A). These data suggest that reduced mitochondrial biogenesis is an early event in the hippocampus of APP/PS1 mice.

3.6. Mitochondrial OXPHOS expression

Deregulation in OXPHOS signaling is indicative of mitochondrial function impairment and has been previously reported in the brains of 3 and 6 month old APP mice [46,47]. In agreement with the above mentioned studies, we have detected a significant reduction in OXPHOS complexes I, II, III, and IV in the hippocampi of the 3 month old APP/PS1 mice (Fig. 5).

3.7. Tau phosphorylation and Tau kinase levels

Since Tau expression is regulated by insulin/IGF-I, and also by AMPK, increased Tau phosphorylation could be an early event in the brains of APP/PS1 mice. It is well-known that Tau is a microtubule-binding protein participating in neuronal cytoskeletal dynamics maintenance and axonal transport [55–59]. Evaluation of several Tau phosphoepitopes by Western blotting, revealed a global increase in Tau phosphorylation in the hippocampal extracts of APP/PS1 mice, both at 3 and 6 months of age (Fig. 6).

3.8. Involvement of GSK-3β and CDK5 kinases in the early stages of the amyloidogenesis and Tau phosphorylation

Insulin and IGFI signaling regulate the expression and phosphorylation of Tau proteins, as impaired insulin function leads to the overactivation of GSK-3β, a kinase capable of Tau phosphorylation. Our results show a significant increase in p35 content and pCDK5 (Tyr15)/CDK5 ratios in the hippocampus of APP/PS1 animals, compared to controls, both at 3 and 6 months of age. In contrast, the protein expression levels of GSK-3β, phosphorylated at Ser9 (inactive form), and Tyr216 (active form), as well as of IDE, remained unchanged (Fig. 7).

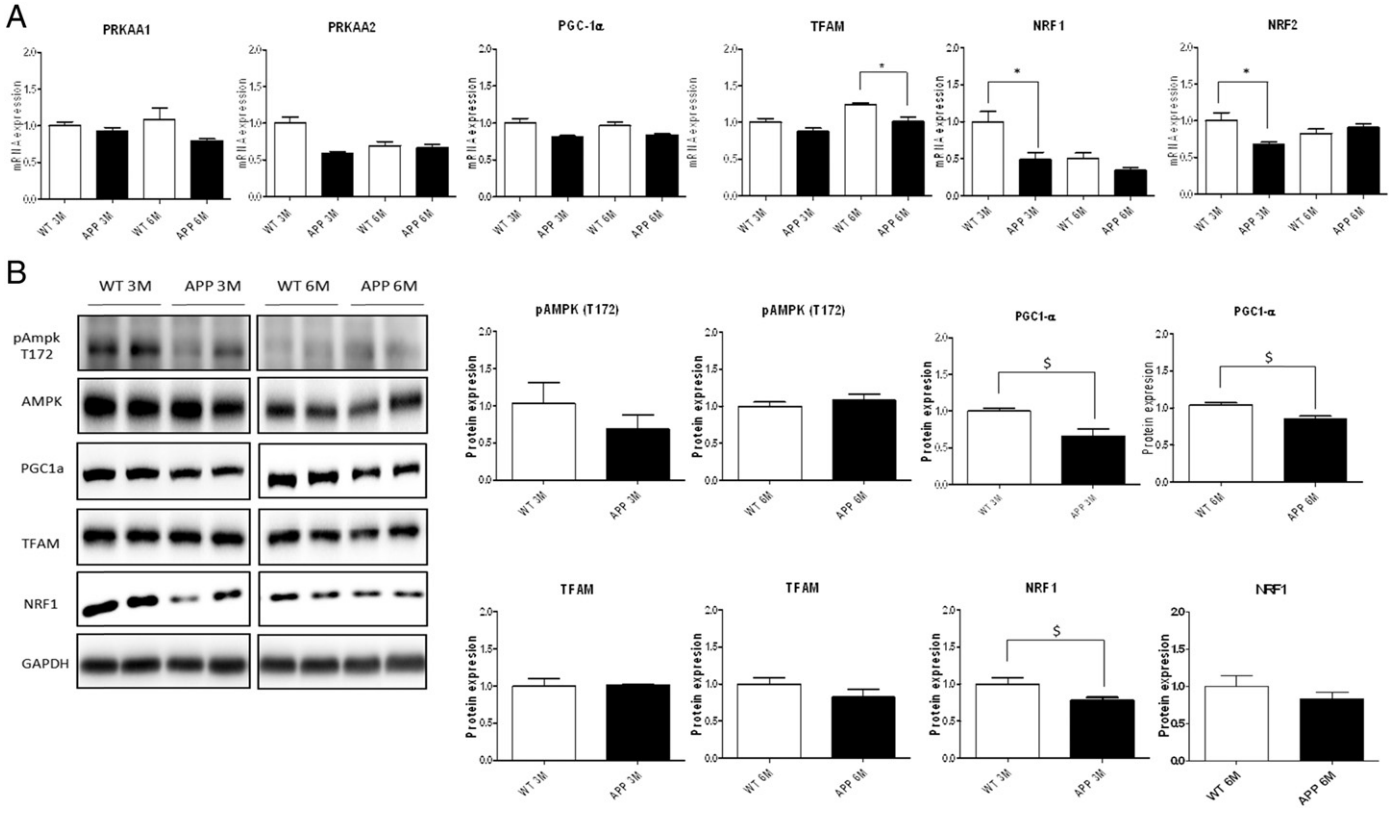

Fig. 4. mRNA expression profile (n = 4–6) (A) and representative immunoblot images and quantification (n = 4–6) (B) of the molecules related to energy metabolism and mitochondrial biogenesis in the hippocampal extracts of 3 and 6 month old wild-type and APP/PS1 mice. pAMPK (T172) is normalized to total AMPK levels, with the rest of the proteins normalized to GAPDH. (Statistical analysis was performed with one-way ANOVA and with Tukey's post-hoc test, where * denotes $p < 0.05$, ** denotes $p < 0.01$, and *** denotes $p < 0.001$, and with the student's t-test, where $ denotes $p < 0.05$).

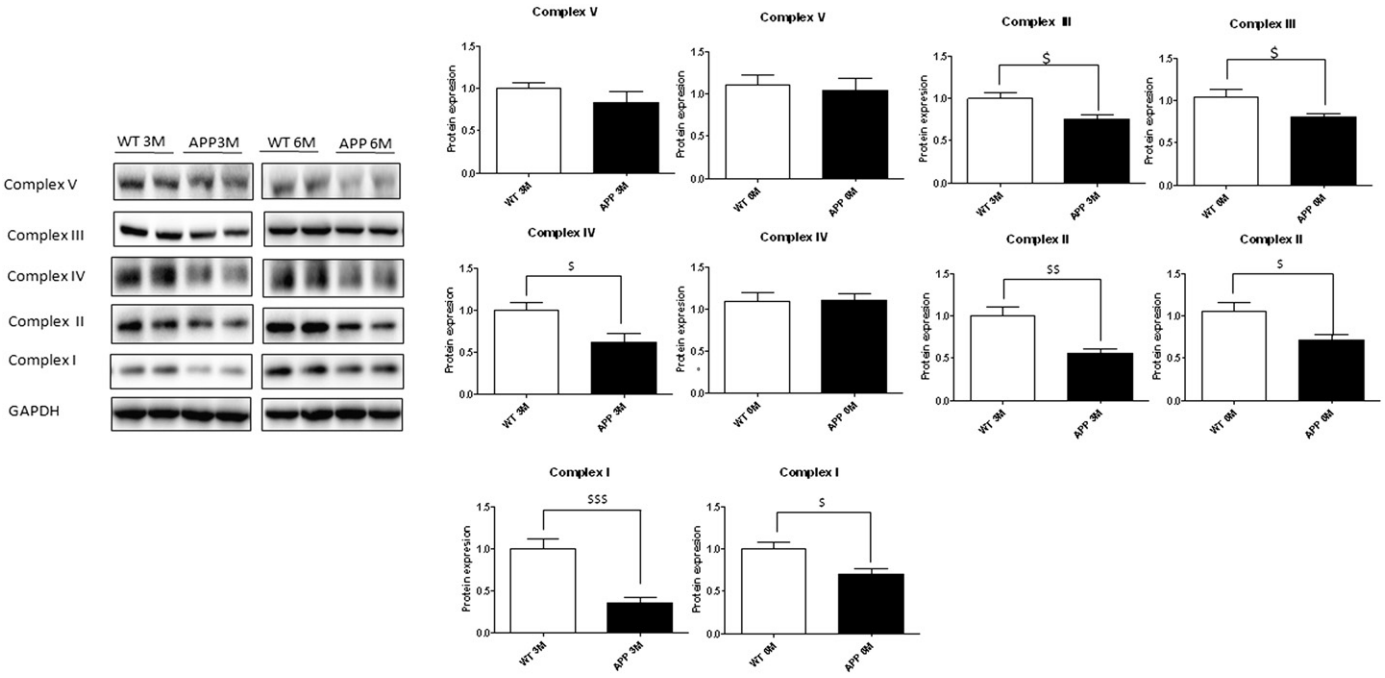

Fig. 5. Representative immunoblot images and quantification of various OXPHOS complexes, normalized to GAPDH protein levels, in the hippocampal extracts of 3 and 6 month old wild-type and APP/PS1 mice (n = 4–6). (Statistical analysis was performed with the student's t-test, where $ denotes $p < 0.05$, $$ denotes $p < 0.01$, and $$$ denotes $p < 0.001$.)

3.9. Changes in synaptic protein levels

Because Aβ oligomers induce synaptic loss in AD we evaluated protein expression levels of representative pre- and post-synaptic proteins (synaptophysin (SYP) and PSD-95 respectively). As shown in Fig. 8, there were no significant changes in their levels in the hippocampus of APP/PS1 mice, relative to the control tissue. Our results are in agreement with a previous study by Minkeviciene et al. who did not detect any changes in synaptic protein levels in 17 month-old APP/PS1 mice [48].

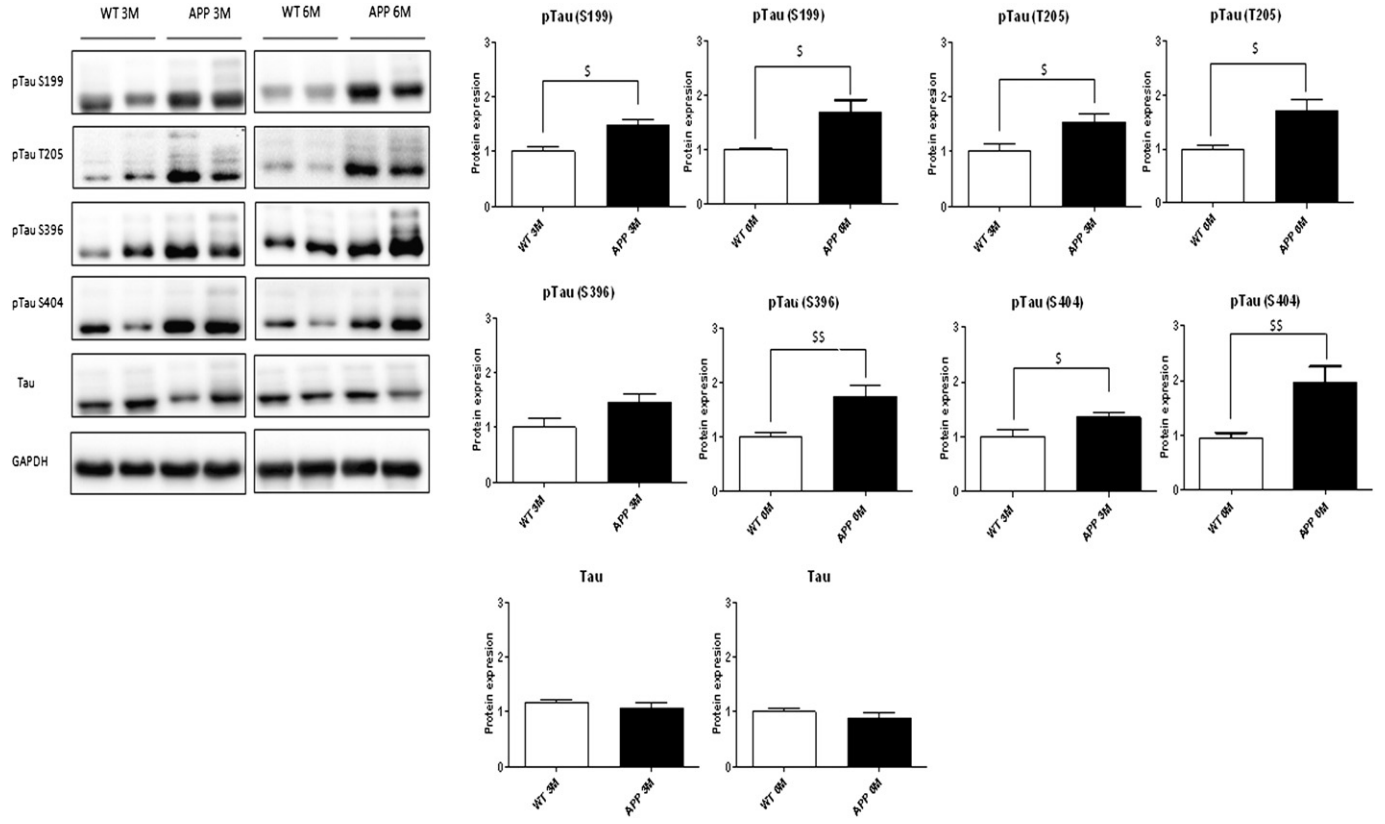

Fig. 6. Representative immunoblot images and quantification of various Tau phosphoepitopes, normalized to total Tau protein levels, in the hippocampal extracts of 3 and 6 month old wild-type and APP/PS1 mice (n = 4–6). (Statistical analysis was performed with the student's t-test, where $ denotes $p < 0.05$ and $$ denotes $p < 0.01$.)

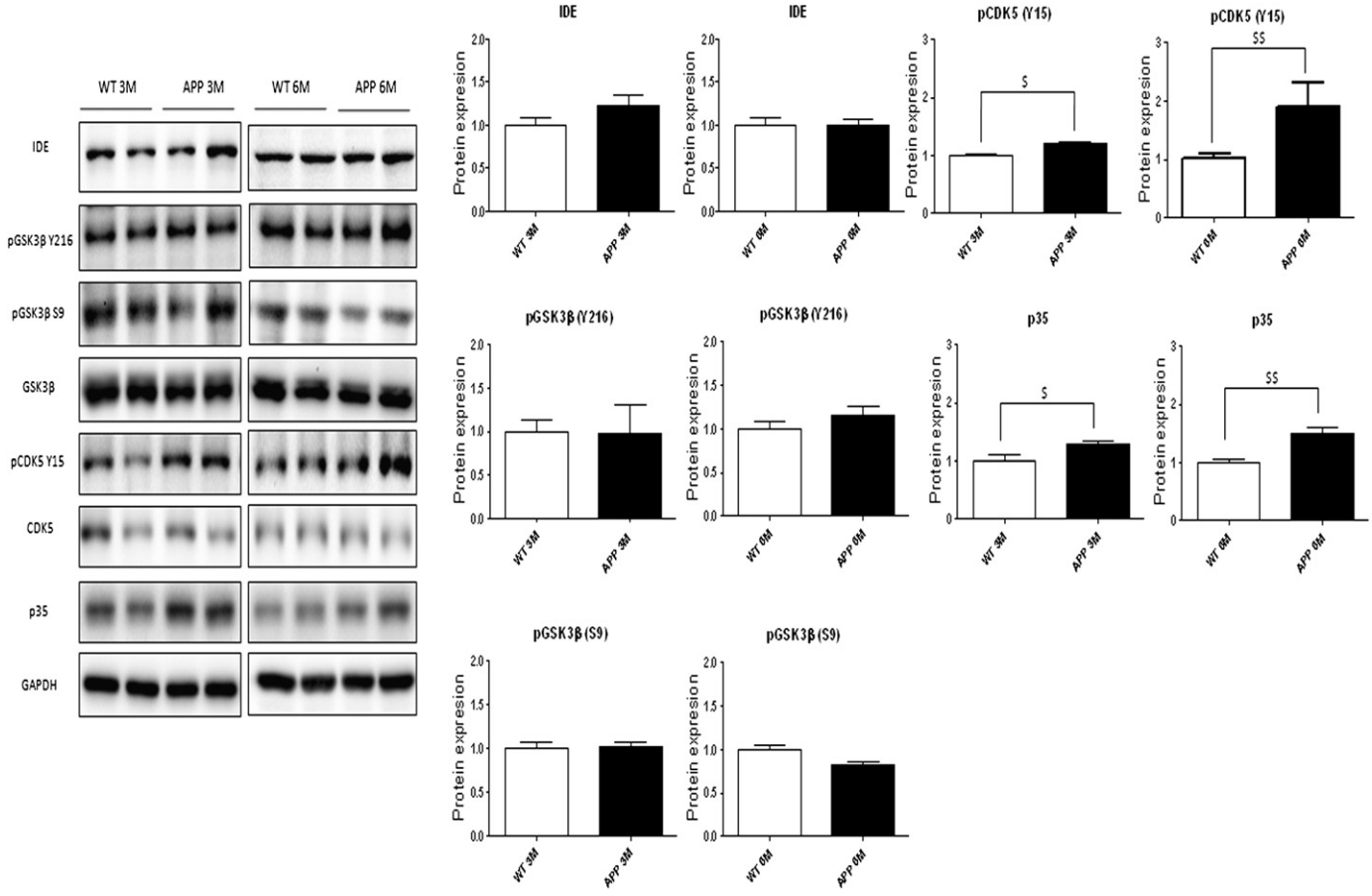

Fig. 7. Representative immunoblot images and quantification of molecules implicated in insulin signaling and Tau phosphorylation, in the hippocampal extracts of 3 and 6 month old wild-type and APP/PS1 mice (n = 4–6). pCDK (Y15), pGSK3β (Y216) and pGSK3β (S9) are normalized to their respective total unphosphorylated protein levels, whereas p35 and IDE are normalized to GAPDH. (Statistical analysis was performed with the student's t-test, where $ denotes $p < 0.05$ and $$ denotes $p < 0.01$.)

4. Discussion

In the current study, we employed an integrated approach consisting of the analyses in both the periphery and at the CNS levels, in order to identify potential changes that occur in the early stages of the amyloidogenic process, prior to amyloid plaque formation in a mouse model of AD. We investigated several key metabolic routes related to glucose uptake and insulin signaling, cellular energy homeostasis, mitochondrial biogenesis and Tau phosphorylation.

In previous studies it was demonstrated that an increase in Aβ levels in APP/PS1 mice is accompanied by plaque deposition in the brain and memory loss, clearly evident at the age of 6 months [11–15]. Thus, APP/PS1 mice are commonly used in AD research [12,14,42,49]. In agreement with these studies, we detected a significant amyloid peptide deposition and the presence of Aβ aggregates in 6 month-old APP/PS1 mice, compared to age-matched wild-type controls. In addition, the 2 object novel object recognition test has revealed a significant cognitive impairment at the age of 6 months in this model. A novel finding in our study is the detection of the insoluble Aβ (1–42) in the brains of 3 month old APP/PS1 mice. This data is intriguing, as Aβ plaques were not detectable by immunohistochemistry at such an early age. Our results suggest that the formation of the insoluble Aβ "proto-fibrils" is

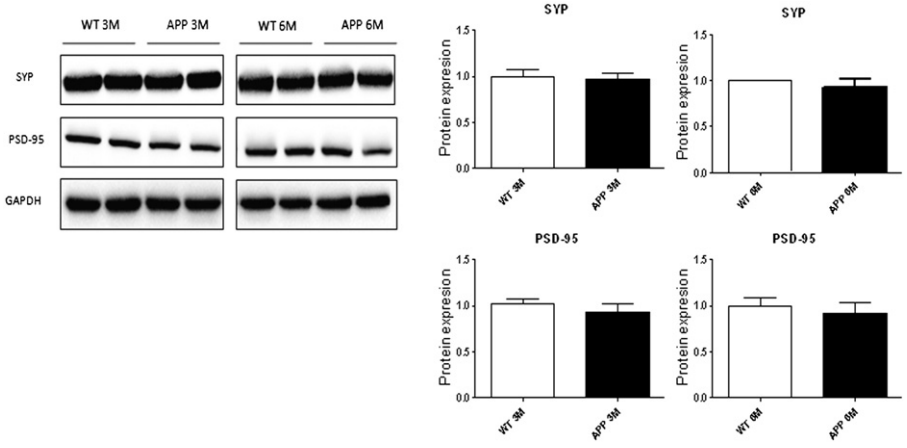

Fig. 8. Representative immunoblot images and quantification of synaptophysin and PSD-95, in the hippocampal extracts of 3 and 6 month old wild-type and APP/PS1 mice (n = 4–6).

an early event which leads to plaque formation by the age of 6 months. Elevated levels of the insoluble Aβ (1–42) were previously reported in brain homogenates of 6 month old APP/PS1 animals [50]. However, the authors of that study did not detect any Aβ in 4 month old mice. The discrepancy with this study could be explained by the differences in experimental methodologies. As expected, by the age of 6 months we have detected a further increase in the levels of insoluble Aβ (1–42) together with the appreciable levels of both soluble and the insoluble Aβ (1–40) as well as senile plaques,

Moreover, in the present research, we demonstrate early changes affecting insulin signaling in the preplaque APP/PS1 mice. These mice display impairment in genes involved in glucose metabolism and mitochondrial function, such as OXPHOS. Thus, as mentioned above, AD neuropathology can be explained, in part, through alterations in glucose metabolism. It was previously published that in 5–7 week-old APP/PS1 mice, glucose and insulin tolerance were not impaired [16]. In our study, we had used older animals and our results demonstrated a tendency towards altered glucose tolerance already at 3 months of age, with the 6-month-old animals exhibiting significantly impaired glucose and insulin tolerance. In the same model, but employing female mice, Hiltunen et al. reported significantly impaired glucose tolerance at 7 months of age in APP/PS1 animals, compared to wild-type controls. Interestingly, the authors did not detect any changes in ITT, but this could be explained by the fact that the ITT was terminated 20 min after the insulin injection. In our study, the biggest differences in ITT between the wild-type and transgenic animals occurred between 30 and 60 min, following i.p. insulin administration. In addition, Hiltunen and colleagues generated triple transgenic mice by cross-breeding APP/PS1 with the mice overexpressing pancreatic IGF2 [49]. While IGF2 single mutants showed impaired glucose and insulin tolerance, in triple APP/PS1/IGF2 animals, this phenotype was further exacerbated. In fact, our results clearly show a significant age-dependent increase in the IGF2 content in the hippocampus, supporting the role of IGF2 signaling in the metabolic perturbations affecting APP/PS1 mice.

Recent studies suggest that there is a close link between insulin-deficient diabetes and cerebral amyloidosis in the pathogenesis of AD [25,51–59]. Using a streptozotocin (STZ)-induced diabetic APP/PS1 mouse model, it has been shown that the diabetic condition promoted the processing of APP, resulting in increased Aβ generation, neuritic plaque formation, and spatial memory deficits [24]. Patients with AD show a remarkable deposition of Aβ peptide in the brain, whereas patients with T2DM present Islet Amyloid Polypeptide (IAPP) deposition in pancreatic β-cells [17]. Then, AD and T2DM share common key molecular alterations in Aβ peptide processing and insulin signaling, in a poorly understood interplay [15–17,51,52,60–65]. Chua and colleagues have suggested that an increase in brain Aβ42 levels in 15 month-old female APP/PS1 mice, may be dependent on impaired brain insulin signaling [53]. However, Sadowski and colleagues demonstrated a correlation between the hippocampal amyloid plaque levels and glucose utilization at 22 months of age. It is of note, that the majority of published studies focus on very late stages of the disease, when Aβ plaques are fully developed [66].

Therefore, the question would be: Are metabolic disorders the cause or the consequence of the AD? It is known that brain glucose metabolism defects are strongly associated with memory impairment in AD brain. Human brain imaging studies indicate that impaired glucose utilization precedes the onset of cognitive deficits in AD, suggesting causality [21]. In this context, the binding of insulin, IRS1 and IRS2 to the INSR, could modulate hippocampal synaptic plasticity and memory consolidation [19–22]. In agreement with this hypothesis, we detected a small, but significant reduction in the hippocampal *Arc*, *Fos*, *Insr* and *Irs2* transcripts in 3 month-old APP/PS1 mice, compared to wild-type controls. By the age of 6 months, APP/PS1 mice develop impaired glucose and insulin tolerance, accompanied by a significant increase in *Igf2* and *Igfbp2* transcripts. Interestingly, we did not detect any changes in the transcription of *Igf1*, which is involved in development, cognitive functions and aging processes, and the alterations of which had been linked to AD pathology.

Downstream of insulin signaling, we focused on mitochondrial markers. Structural and functional perturbations of mitochondria in AD have been recognized for some time, and led Swerdlow and Khan to propose the mitochondrial cascade hypothesis [5]. This hypothesis states that inherited mutations in mitochondrial DNA determine the basal functional ability of mitochondria to respond to, and to recover from stress-induced signaling. The physiopathology of AD develops when the mitochondria lose their functional capacity, and includes neuronal apoptosis, Aβ deposition, and neurofibrillary tangles [7,59–65]. Here, we report a significant downregulation in mitochondrial OXPHOS complexes in the brains of 3 month old APP/PS1 mice. Likewise, we detected reduced mRNA expression levels of genes related to mitochondrial biogenesis and the regulation of energy metabolism, including *Prkaa2* subunit of AMPK, *Pgc-1α*, *Nrf1* and *Nrf2*. NRF1, through its interaction with PGC-1α, regulates mitochondrial biogenesis directly, and is a key transcriptional regulator of IDE [62–64]. The vast majority of IDE protein is localized to the cytosol, with the small amounts present in the mitochondria, where it participates in Aβ degradation. Mitochondrial localization is dependent on the long isoform of ide mRNA transcripts, the expression of which was found to be positively correlated with *Pgc-1α* and *Nrf-1* transcripts in the brains of non-demented human patients. Interestingly, the correlation was weaker in the brains of AD patients, suggesting an impairment of this route [49]. The observed reduction of *Pgc-1α* and *Nrf-1*, both at the mRNA and protein levels, in the hippocampi of young APP/PS1 animals in our study, supports this hypothesis. The lack of changes in IDE protein levels can be explained by the phenomenon of eclipsed distribution [63]. As the dominant, short isoform of IDE is ubiquitously expressed in the cytosol, any changes at the mitochondrial level would be masked by this dominant isoform.

PGC-1α is a member of a family of transcriptional coactivators that plays a central role in the regulation of cellular energy metabolism. It stimulates mitochondrial biogenesis and participates in the regulation of both carbohydrate and lipid metabolism in peripheral disorders such as obesity and diabetes, however its role in the CNS is less clear [55–60]. In addition to the direct effects on mitochondrial gene expression, PGC-1α is also involved in the regulation of genes that protect neuronal cells from oxidative stress, such as mitochondrial superoxide dismutase. PGC-1α is regulated by several metabolism-responsive elements like AMPK which, when activated by elevated AMP/ATP ratios, can phosphorylate it directly [59]. Recent reports indicate that PGC-1α could be a potential biomarker of AD disease, as reduced PGC-1α mRNA and protein levels had been detected in AD brains [58–61]. In agreement with this, we detected significant reductions in PGC-1α mRNA and protein levels in APP/PS1 brains, compared to wild-type controls, at 3 and 6 months of age. We also observed a decrease in a ratio of activated pAMPK (Thr172)/Total APMK in 3 month old APP/PS1 mice, supporting the role of mitochondrial biogenesis impairment in the early stages of AD. PGC-1α remains an attractive target for AD therapeutic intervention [59].

AMPK is a cellular energy sensor conserved in all eukaryotic cells. It regulates the activities of a number of key metabolic enzymes and protects cells from stresses that cause ATP depletion, by switching off ATP-consuming biosynthetic pathways [58]. It AMPK can also phosphorylate substrates like Tau proteins, thereby causing their hyperphosphorylation. Tau hyperphosphorylation occurs both as a result of elevated levels of Aβ and genetic mutations in Tau proteins, and causes microtubule disassembly, which leads to the formation of neurofibrillary tangles and synaptic loss. In a mouse model overexpressing a P301L-mutated version of human Tau (rTgP301L transgene), Tau hyperphosphorylation resulted in its accumulation in the still functional dendritic spines. Significantly, these observations were reported in relatively young 4.5 month-old animals, at an age when cognitive impairments were already evident, but neither the neuronal, nor synaptic loss was detectable [61].

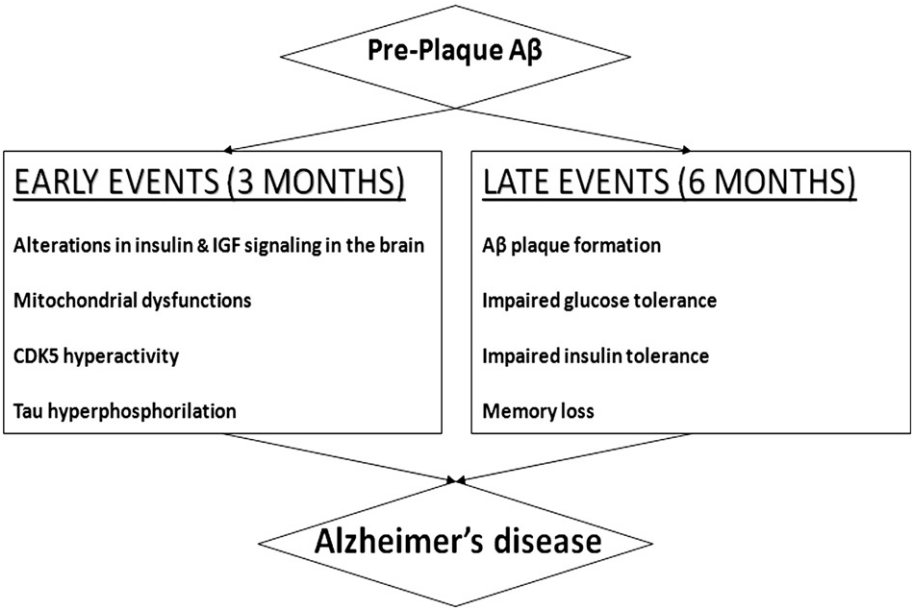

Fig. 9. Summary of the events, leading to the progressive amyloid plaque deposition and memory loss in an APP/PS1 mouse model of FAD.

We detected a significant increase in phosphorylation of several Tau phosphoepitopes in the hippocampi of APP/PS1 mice, compared to controls, including p-Tau (Ser199); p-Tau (Ser 205); p-Tau (Ser 396); and p-Tau (Ser404). At the same time, the protein levels of phosphorylated forms of AMPK and GSK-3β remained unchanged, suggesting that Tau phosphorylation occurs via an alternative pathway in our model. Several studies have suggested that AD and T2DM may share a common pathway to pathology: the hyperactivation of CDK5 [67–69]. CDK5 activation may cause aberrant phosphorylation of cytoskeletal components like Tau and neurofilaments. Results from our research demonstrated an increase in p(Y15) CDK5 phosphorylation in 3 and 6 month-old APP/PS1 mice, suggesting that CDK5 may be the kinase involved in Tau phosphorylation [62,64–71].

In summary, our results show an early downregulation of glucose, insulin signaling and energy metabolism pathways in an APP/PS1 mouse model of FAD. An overview of the key events, occurring between 3 and 6 months of age in our model, is presented in Fig. 9. These changes affect the activity of key molecules involved in memory processes (Arc, Fos) and mitochondrial regulation, such as OXPHOS, PGC-1α and NRF1, as well as Tau phosphorylation. The data presented here reinforces the hypothesis that the preceding events in the amyloidogenenic process in AD are related to both insulin signaling and energy metabolism impairment. Finally, we demonstrate an increase in the levels of pCDK5, which may be responsible for Tau phosphorylation and NFT formation in the hippocampi of the APP/PS1 mice.

Acknowledgments

This study was funded by grant 2009/SGR00853 from the Generalitat de Catalunya (autonomous government of Catalonia), by grants BFU2010-19119/BFI, SAF2011-23631, SAF2012-39852-C02-01 and SAF2012-30708 from the Spanish Ministerio de Ciencia e Innovación and grant 0177594 from the CONACYT (Mexico).

References

[1] M.A. Smith, Alzheimer disease, Int. Rev. Neurobiol. 42 (1998) 1–54.
[2] J. Hardy, D.J. Selkoe, The amyloid hypothesis of Alzheimer's disease: progress and problems on the road to therapeutics, Science 297 (2002) 353–356.
[3] J.A. Hardy, G.A. Higgins, Alzheimer's disease: the amyloid cascade hypothesis, Science 256 (1992) 184–185.
[4] A. Erol, An integrated and unifying hypothesis for the metabolic basis of sporadic Alzheimer's disease, J. Alzheimers Dis. 13 (2008) 241–253.
[5] R.H. Swerdlow, S.M. Khan, A "mitochondrial cascade hypothesis" for sporadic Alzheimer's disease, Med. Hypotheses 63 (2004) 8–20.
[6] N. Bassil, G.T. Grossberg, Novel regimens and delivery systems in the pharmacological treatment of Alzheimer's disease, CNS Drugs 23 (2009) 293–307.
[7] R.H. Swerdlow, Mitochondria and cell bioenergetics: increasingly recognized components and a possible etiologic cause of Alzheimer's disease, Antioxid. Redox Signal. 16 (2012) 1434–1455.
[8] W. Zhang, J. Hao, R. Liu, Z. Zhang, G. Lei, C. Su, J. Miao, Z. Li, Soluble Aβ levels correlate with cognitive deficits in the 12-month-old APPswe/PS1dE9 mouse model of Alzheimer's disease, Behav. Brain Res. 222 (2011) 342–350.
[9] J.E. Selfridge, J. Lu, R.H. Swerdlow, Role of mitochondrial homeostasis and dynamics in Alzheimer's disease, Neurobiol. Dis. 51 (2013) 3–12.
[10] S.W. Pimplikar, Reassessing the amyloid cascade hypothesis of Alzheimer's disease, Int. J. Biochem. Cell Biol. 41 (2009) 1261–1268.
[11] S.W. Pimplikar, R.A. Nixon, N.K. Robakis, J. Shen, L.H. Tsai, Amyloid-independent mechanisms in Alzheimer's pathogenesis, J. Neurosci. 30 (2010) 14946–14954.
[12] W. Zhang, M. Bai, Y. Xi, J. Hao, L. Liu, N. Mao, C. Su, J. Miao, Z. Li, Early memory deficits precede plaque deposition in APPswe/PS1dE9 mice: involvement of oxidative stress and cholinergic dysfunction, Free Radic. Biol. Med. 52 (2012) 1443–1452.
[13] N. Sato, R. Morishita, Plasma β-amyloid: a possible missing link between Alzheimer disease and diabetes, Diabetes 62 (2013) 1005–1006.
[14] W. Zhang, M. Bai, Y. Xi, J. Hao, Z. Zhang, C. Su, G. Lei, J. Miao, Z. Li, Multiple inflammatory pathways are involved in the development and progression of cognitive deficits in APPswe/PS1dE9 mice, Neurobiol. Aging 33 (2012) 2661–2677.
[15] F.G. De Felice, Alzheimer's disease and insulin resistance: translating basic science into clinical applications, J. Clin. Invest. 123 (2013) 531–539.
[16] M. Jiménez-Palomares, J.J. Ramos-Rodríguez, J.F. López-Acosta, M. Pacheco-Herrero, A.M. Lechuga-Sancho, G. Perdomo, M. García-Alloza, I. Cózar-Castellano, Increased Aβ production prompts the onset of glucose intolerance and insulin resistance, Am. J. Physiol. Endocrinol. Metab. 302 (2012) E1373–E1380.
[17] L. Haataja, T. Gurlo, C.J. Huang, P.C. Butler, Islet amyloid in type 2 diabetes, and the toxic oligomer hypothesis, Endocr. Rev. 29 (2008) 303–316.
[18] Y. Zhang, B. Zhou, F. Zhang, J. Wu, Y. Hu, Y. Liu, Q. Zhai, Amyloid-β induces hepatic insulin resistance by activating JAK2/STAT3/SOCS-1 signaling pathway, Diabetes 61 (2012) 1434–1443.
[19] S.M. de la Monte, Brain insulin resistance and deficiency as therapeutic targets in Alzheimer's disease, Curr. Alzheimer Res. 9 (2012) 35–66.
[20] M.C. Leal, N. Magnani, S. Villordo, C.M. Buslje, P. Evelson, E.M. Castaño, L. Morelli, Transcriptional regulation of insulin-degrading enzyme modulates mitochondrial amyloid β (Aβ) peptide catabolism and functionality, J. Biol. Chem. 288 (2013) 12920–12931.
[21] S.M. de la Monte, Contributions of brain insulin resistance and deficiency in amyloid-related neurodegeneration in Alzheimer's disease, Drugs 72 (2012) 49–66.
[22] de la Monte, J.R. Wands, Alzheimer's disease is type 3 diabetes—evidence reviewed, J. Diabetes Sci. Technol. 2 (2008) 1101–1113.

[23] A. Trueba-Sáiz, C. Cavada, A.M. Fernandez, T. Leon, D.A. González, J. Fortea Ormaechea, A. Lleó, T. Del Ser, A. Nuñez, I. Torres-Aleman, Loss of serum IGF-I input to the brain as an early biomarker of disease onset in Alzheimer mice, Transl. Psychiatry 3 (Dec 3 2013) e330.
[24] X. Wang, W. Zheng, J.W. Xie, T. Wang, S.L. Wang, W.P. Teng, Z.Y. Wang, Insulin deficiency exacerbates cerebral amyloidosis and behavioral deficits in an Alzheimer transgenic mouse model, Mol. Neurodegener. 2 (2010) 46.
[25] N. Sato, R. Morishita, Roles of vascular and metabolic components in cognitive dysfunction of Alzheimer disease: short- and long-term modification by non-genetic risk factors, Front. Aging Neurosci. 5 (2013) 64.
[26] E. van Exel, P. Eikelenboom, H. Comijs, D.J. Deeg, M.L. Stek, R.G. Westendorp, Insulin-like growth factor-1 and risk of late-onset Alzheimer's disease: findings from a family study, Neurobiol. Aging 35 (2014) 725.e7–725.e10.
[27] E. Steen, B.M. Terry, E.J. Rivera, J.L. Cannon, T.R. Neely, R. Tavares, X.J. Xu, J.R. Wands, S.M. de la Monte, Impaired insulin and insulin-like growth factor expression and signaling mechanisms in Alzheimer's disease—is this type 3 diabetes? J. Alzheimers Dis. 7 (2005) 63–80.
[28] W. Farris, S. Mansourian, Y. Chang, L. Lindsley, E.A. Eckman, M.P. Frosch, Insulin-degrading enzyme regulates the levels of insulin, amyloid beta-protein, and the beta-amyloid precursor protein intracellular domain in vivo, Proc. Natl. Acad. Sci. U. S. A. 100 (2003) 4162–4167.
[29] S. Takeda, N. Sato, H. Rakugi, R. Morishita, Molecular mechanisms linking diabetes mellitus and Alzheimer disease: beta-amyloid peptide, insulin signaling, and neuronal function, Mol. Biosyst. 7 (2011) 1822–1827.
[30] S. Takeda, N. Sato, K. Uchio-Yamada, K. Sawada, T. Kunieda, D. Takeuchi, H. Kurinami, M. Shinohara, H. Rakugi, R. Morishita, Elevation of plasma beta-amyloid level by glucose loading in Alzheimer mouse models, Biochem. Biophys. Res. Commun. 385 (2009) 193–197.
[31] B.K. Binukumar, Y.L. Zheng, V. Shukla, N.D. Amin, P. Grant, H.C. Pant, TFP5, a peptide derived from p35,a CDK5 neuronal activator, rescues cortical neurons from glucose toxicity, J. Alzheimers Dis. 39 (2014) 899–909.
[32] J.L. Hallows, K. Chen, R.A. DePinho, I. Vincent, Decreased cyclin-dependent kinase 5 (CDK5) activity is accompanied by redistribution of CDK5 and cytoskeletal proteins and increased cytoskeletal protein phosphorylation in p35 null mice, J. Neurosci. 23 (2003) 10633–10644.
[33] M. Takahashi, E. Iseki, K. Kosaka, CDK5 and munc-18/p67 colocalization in early stage neurofibrillary tangles-bearing neurons in Alzheimer type dementia brains, J. Neurol. Sci. 172 (2000) 63–69.
[34] D. Alvira, I. Ferrer, J. Gutierrez-Cuesta, B. Garcia-Castro, M. Pallàs, A. Camins, Activation of the calpain/CDK5/p25 pathway in the girus cinguli in Parkinson's disease, Parkinsonism Relat. Disord. 14 (2008) 309–313.
[35] A. Camins, E. Verdaguer, J. Folch, A.M. Canudas, M. Pallàs, The role of CDK5/P25 formation/inhibition in neurodegeneration, Drug News Perspect. 19 (2006) 453–460.
[36] D.S. Smith, L.H. Tsai, CDK5 behind the wheel: a role in trafficking and transport? Trends Cell Biol. 12 (2002) 28–36.
[37] S. Bandyopadhyay, X. Huang, D.K. Lahiri, J.T. Rogers, Novel drug targets based on metallobiology of Alzheimer's disease, Expert Opin. Ther. Targets 14 (2010) 1177–1197.
[38] E.M. Blalock, K.C. Chen, A.J. Stromberg, C.M. Norris, I. Kadish, S.D. Kraner, N.M. Porter, P.W. Landfield, Harnessing the power of gene microarrays for the study of brain aging and Alzheimer's disease: statistical reliability and functional correlation, Ageing Res. Rev. 4 (2005) 481–512.
[39] A.L. Barabasi, Z.N. Oltvai, Network biology: understanding the cell's functional organization, Nat. Rev. Genet. 5 (2004) 101–113.
[40] E.M. Blalock, K.C. Chen, K. Sharrow, J.P. Herman, N.M. Porter, T.C. Foster, P.W. Landfield, Gene microarrays in hippocampal aging: statistical profiling identifies novel processes correlated with cognitive impairment, J. Neurosci. 23 (2003) 3807–3819.
[41] J.T. Dou, M. Chen, F. Dufour, D.L. Alkon, W.Q. Zhao, Insulin receptor signaling in long-term memory consolidation following spatial learning, Learn. Mem. 12 (2005) 646–655.
[42] E. Aso, S. Lomoio, I. López-González, L. Joda, M. Carmona, N. Fernández-Yagüe, J. Moreno, S. Juvés, A. Pujol, R. Pamplona, M. Portero-Otin, V. Martín, M. Díaz, I. Ferrer, Amyloid generation and dysfunctional immunoproteasome activation with disease progression in animal model of familial Alzheimer's disease, Brain Pathol. 22 (2012) 636–653.
[43] E. Barroso, J. del Valle, D. Porquet, A.M. Vieira Santos, L. Salvadó, R. Rodríguez-Rodríguez, P. Gutiérrez, M. Anglada-Huguet, J. Alberch, A. Camins, X. Palomer, M. Pallàs, L. Michalik, W. Wahli, M. Vázquez-Carrera, Tau hyperphosphorylation and increased BACE1 and RAGE levels in the cortex of PPARβ/δ-null mice, Biochim. Biophys. Acta 1832 (2013) 1241–1248.
[44] E. Masliah, E. Rockenstein, I. Veinbergs, Y. Sagara, M. Mallory, M. Hashimoto, L. Mucke, Beta-amyloid peptides enhance alpha-synuclein accumulation and neuronal deficits in a transgenic mouse model linking Alzheimer's disease and Parkinson's disease, Proc. Natl. Acad. Sci. U. S. A. 98 (2001) 12245–12250.
[45] C.A. Dickey, M.N. Gordon, J.E. Mason, N.J. Wilson, D.M. Diamond, J.F. Guzowski, D. Morgan, Amyloid suppresses induction of genes critical for memory consolidation in APP + PS1 transgenic mice, J. Neurochem. 88 (2004) 434–442.
[46] S. Hauptmann, I. Scherping, S. Dröse, U. Brandt, K.L. Schulz, M. Jendrach, K. Leuner, A. Eckert, W.E. Müller, Mitochondrial dysfunction: an early event in Alzheimer pathology accumulates with age in AD transgenic mice, Neurobiol. Aging 30 (2009) 1574–1586.
[47] A. Eckert, K.L. Schulz, V. Rhein, J. Götz, Convergence of amyloid-beta and tau pathologies on mitochondria in vivo, Mol. Neurobiol. 41 (2010) 107–114.
[48] R. Minkeviciene, J. Ihalainen, T. Malm, O. Matilainen, V. Keksa-Goldsteine, G. Goldsteins, H. Iivonen, N. Leguit, J. Glennon, J. Koistinaho, P. Banerjee, H. Tanila, Age-related decrease in stimulated glutamate release and vesicular glutamate transporters in APP/PS1 transgenic and wild-type mice, J. Neurochem. 105 (2008) 584–594.
[49] M. Hiltunen, V.K. Khandelwal, N. Yaluri, T. Tiilikainen, M. Tusa, H. Koivisto, M. Krzisch, S. Vepsäläinen, P. Mäkinen, S. Kemppainen, P. Miettinen, A. Haapasalo, H. Soininen, M. Laakso, H. Tanila, Contribution of genetic and dietary insulin resistance to Alzheimer phenotype in APP/PS1 transgenic mice, J. Cell. Mol. Med. 16 (2012) 1206–1222.
[50] M. Garcia-Alloza, E.M. Robbins, S.X. Zhang-Nunes, S.M. Purcell, R.A. Betensky, S. Raju, C. Prada, S.M. Greenberg, B.J. Bacskai, M.P. Frosch, Characterization of amyloid deposition in the APPswe/PS1dE9 mouse model of Alzheimer disease, Neurobiol. Dis. 24 (2006) 516–524.
[51] M. Hokama, S. Oka, J. Leon, T. Ninomiya, H. Honda, K. Sasaki, T. Iwaki, T. Ohara, T. Sasaki, F.M. Laferla, Y. Kiyohara, Y. Nakabeppu, Altered expression of diabetes-related genes in Alzheimer's disease brains: the Hisayama study, Cereb. Cortex (2013) in press. http://dx.doi.org/10.1093/cercor/bht101 .
[52] J.J. Ramos-Rodriguez, O. Ortiz, M. Jimenez-Palomares, K.R. Kay, E. Berrocoso, M.I. Murillo-Carretero, G. Perdomo, T. Spires-Jones, I. Cozar-Castellano, A.M. Lechuga-Sancho, M. Garcia-Alloza, Differential central pathology and cognitive impairment in pre-diabetic and diabetic mice, Psychoneuroendocrinology 38 (2013) 2462–2475.
[53] L.M. Chua, M.L. Lim, P.R. Chong, Z.P. Hu, N.S. Cheung, B.S. Wong, Impaired neuronal insulin signaling precedes Aβ42 accumulation in female AβPPsw/PS1ΔE9 mice, J. Alzheimers Dis. 29 (2012) 783–791.
[54] U. Andersson, R.C. Scarpulla, Pgc-1-related coactivator, a novel, serum-inducible coactivator of nuclear respiratory factor 1-dependent transcription in mammalian cells, Mol. Cell. Biol. 21 (2001) 3738–3749.
[55] B.N. Finck, D.P. Kelly, PGC-1 coactivators: inducible regulators of energy metabolism in health and disease, J. Clin. Invest. 116 (2006) 615–622.
[56] B. Sheng, X. Wang, B. Su, H.G. Lee, G. Casadesus, G. Perry, X. Zhu, Impaired mitochondrial biogenesis contributes to mitochondrial dysfunction in Alzheimer's disease, J. Neurochem. 120 (2012) 419–429.
[57] L. Katsouri, C. Parr, N. Bogdanovic, M. Willem, M. Sastre, PARγ co-activator-1α (PGC-1α) reduces amyloid-β generation through a PPARγ-dependent mechanism, J. Alzheimers Dis. 25 (2011) 151–162.
[58] N.A. Shirwany, M.H. Zou, AMPK: a cellular metabolic and redox sensor. A minireview, Front. Biosci. (Landmark Ed.) 19 (2014) 447–474.
[59] D. Kim, M.D. Nguyen, M.M. Dobbin, A. Fischer, F. Sananbenesi, J.T. Rodgers, I. Delalle, J.A. Baur, G. Sui, S.M. Armour, P. Puigserver, D.A. Sinclair, L.H. Tsai, SIRT1 deacetylase protects against neurodegeneration in models for Alzheimer's disease and amyotrophic lateral sclerosis, EMBO J. 26 (2007) 3169–3179.
[60] W. Qin, V. Haroutunian, P. Katsel, C.P. Cardozo, L. Ho, J.D. Buxbaum, G.M. Pasinetti, PGC-1alpha expression decreases in the Alzheimer disease brain as a function of dementia, Arch. Neurol. 66 (2009) 352–361.
[61] L. Galluzzi, K. Blomgren, G. Kroemer, Mitochondrial membrane permeabilization in neuronal injury, Nat. Rev. Neurosci. 10 (2009) 481–494.
[62] B.R. Hoover, N.R.M. Reed, S. Jianjun, R.D. Penrod, L.A. Kotilinek, M.K. Grant, R. Pitstick, Tau mislocalization to dendritic spines mediates synaptic dysfunction independently of neurodegeneration, Neuron 6 (2010) 1067–1081.
[63] V. Shukla, S. Skuntz, H.C. Pant, Deregulated CDK5 activity is involved in inducing Alzheimer's disease, Arch. Med. Res. 43 (2012) 655–662.
[64] L. Zhang, D. Qingyang, W. Zhao, Nuclear respiratory factor 1 mediates the transcription initiation of insulin-degrading enzyme in a TATA box-binding protein-independent manner, PLoS One 8 (2012) e42035.
[65] C.X. Gong, K. Iqbal, Hyperphosphorylation of microtubule-associated protein tau: a promising therapeutic target for Alzheimer disease, Curr. Med. Chem. 15 (2008) 2321–2328.
[66] M. Jucker, L.C. Walker, Self-propagation of pathogenic protein aggregates in neurodegenerative diseases, Nature 501 (2013) 45–51.
[67] M. Sadowski, J. Pankiewicz, H. Scholtzova, Y. Ji, D. Quartermain, C.H. Jensen, K. Duff, R.A. Nixon, R.J. Gruen, T. Wisniewski, Amyloid-beta deposition is associated with decreased hippocampal glucose metabolism and spatial memory impairment in APP/PS1 mice, J. Neuropathol. Exp. Neurol. 63 (2004) 418–428.
[68] N. Regev-Rudzki, O. Pines, Eclipsed distribution: a phenomenon of dual targeting of protein and its significance, Bioessays 29 (2007) 772–782.
[69] A. Vignini, A. Giulietti, L. Nanetti, F. Raffaelli, L. Giusti, L. Mazzanti, L. Provinciali, Alzheimer's disease and diabetes: new insights and unifying therapies, Curr. Diabetes Rev. 9 (2013) 218–227.
[70] Y. Yoshiyama, V.M. Lee, J.Q. Trojanowski, Therapeutic strategies for tau mediated neurodegeneration, J. Neurol. Neurosurg. Psychiatry 84 (2013) 784–795.
[71] K.J. Kopeikina, B.T. Hyman, T.L. Spires-Jones, Soluble forms of tau are toxic in Alzheimer's disease, Transl. Neurosci. 3 (2012) 223–233.
[72] J.E. Ayala, V.T. Samuel, G.J. Morton, S. Obici, C.M. Croniger, G.I. Shulman, D.H. Wasserman, O.P. McGuinness, NIH Mouse Metabolic Phenotyping Center Consortium, Dis Model Mech. 3 (2010) 525–534.
[73] P. Chomczynski, N. Sacchi, Single-step method of RNA isolation by acid guanidinium thiocyanate-phenol-chloroform extraction, Anal Biochem. 162 (1987) 156–159.